The Journal of Experimental Biology 214, 2988-2993

doi:10.1242/jeb.055996

RESEARCH ARTICLE

Humidity affects the extensibility of an orb-weaving spider's viscous thread droplets

Brent D. Opell*, Shannon E. Karinshak and Mary A. Sigler
Department of Biological Sciences, Virginia Tech, Blacksburg, VA 24061, USA
*Author for correspondence (bopell@vt.edu)

Accepted 28 May 2011

SUMMARY

The prey-capture threads found in most spider orb webs rely on viscous droplets for their stickiness. Each droplet is formed of a central mass of viscoelastic glycoprotein glue surrounded by an aqueous covering, both of which incorporate hydrophilic components. We found that the extensibility of droplets on *Larinioides cornutus* threads increased as humidity increased. However, the deflection of the droplets' supporting axial lines did not change, indicating that atmospheric water uptake increases glycoprotein plasticity, but not glycoprotein adhesion. The extensibility of droplets, along with that of the thread's supporting axial fibers, is responsible for summing the adhesion of multiple thread droplets. Therefore, daily changes in humidity have the potential to significantly alter the performance of viscous threads and orb webs.

Key words: Araneoidea, biomaterial, glycoprotein, hygroscopic, *Larinioides cornutus*.

INTRODUCTION

Biological materials function in environments where seasonal and even daily changes in conditions have the potential to alter the properties and performance of these materials. This study is the first to examine how changes in environmental humidity affect the extensibility of droplets, which are responsible for the adhesion of viscous capture threads that are produced by over 4000 species of orb-weaving spiders in the Araneoidea clade (Platnick, 2011). These threads form an orb web's sticky prey capture spiral, which retains insects that strike the web, providing a spider with more time to locate and subdue their prey (Chacón and Eberhard, 1980; Blackledge and Zevenbergen, 2006). Viscous threads are comprised of small, regularly spaced aqueous droplets that surround a pair of supporting axial fibers (Fig. 1a) (Peters, 1986; Vollrath et al., 1990; Vollrath and Tillinghast, 1991; Vollrath, 1992; Tillinghast et al., 1993) and are produced by a triad of spigots on each of a spider's paired posterior spinnerets (Coddington, 1989). The single flagelliform gland spigot of this triad produces an axial fiber and is flanked by two aggregate gland spigots, which coat this fiber with aqueous material. The coated axial fibers merge to form a contiguous pair of fibers surrounded initially by a sheath of viscous material. As a thread absorbs atmospheric moisture in the high humidity of the early morning hours, this material quickly condenses into a regular series of droplets (Edmonds and Vollrath, 1992), whose size and spacing differ greatly among species (Agnarsson and Blackledge, 2009; Opell and Hendricks, 2009; Sensenig et al., 2010).

The glycoprotein within each droplet that confers thread adhesion (Vollrath and Tillinghast, 1991; Tillinghast et al., 1993; Peters, 1995; Opell and Hendricks, 2010) is encoded by two genes (Choresh et al., 2009). The *asg1* gene produces a 406-amino-acid protein, whose upstream region has a high proportion of charged amino acids, which are considered hydrophilic, and its repeating downstream region is similar to mucin, known to have adhesive properties. The *asg2* gene produces a 714-amino-acid protein, whose upstream region is similar to known chitin-binding proteins, adapting it to adhere to insect exoskeleton, whereas its repeating downstream region has high proline content that resembles that of elastin and flagelliform spider silk, making it elastic. This combination of features confers adhesion, extensibility and hygroscopicity to the glycoprotein – crucial and complementary properties in the context viscous thread performance.

A droplet's glycoprotein is surrounded by an aqueous coat (Fig. 1b) (Opell and Hendricks, 2010), which contains hydrophilic low molecular weight compounds (LMWCs) (Vollrath et al., 1990; Townley et al., 1991; Edmonds and Vollrath, 1992), allowing thread droplets to harvest atmospheric moisture and remain hydrated during drier parts of the day (Fig. 2). Although most of a thread's aggregate gland material is consolidated into droplets, a sheath of aqueous material covers axial fibers in inter-droplet regions. This serves to hydrate these fibers, maintaining their super-contracted state and increasing their tension (Work, 1981; Work, 1982; Vollrath and Edmonds, 1989; Edmonds and Vollrath, 1992; Gosline et al., 1994; Savage and Gosline, 2008; Guinea et al., 2010). This mechanism helps maintain web tension and better equips an orb web to absorb the force of an insect strike (Vollrath and Edmonds, 1989; Edmonds and Vollrath, 1992).

When force is applied to a thread whose droplets have adhered to a surface, its outer droplets elongate more than its inner droplets and the configuration of the axial bridge line approximates a parabola. This conformation sums the adhesion of multiple droplets and implements what has been termed a suspension bridge mechanism (Opell and Hendricks, 2007; Opell and Hendricks, 2009; Opell and Hendricks, 2010; Opell et al., 2008). This mechanism relies on the complementary extensibilities of the thread's axial fibers (Blackledge and Hayashi, 2006a; Blackledge and Hayashi, 2006b; Swanson et al., 2007; Agnarrson and Blackledge, 2009) and the viscoelastic glycoprotein within droplets (Sahni et al., 2010).

As atmospheric humidity changes over the course of a day (Fig. 2), so too does the volume of thread droplets (Vollrath et al., 1990; Townley et al., 1991; Edmonds and Vollrath, 1992). Because the glycoprotein molecules within droplets contain charged amino acids

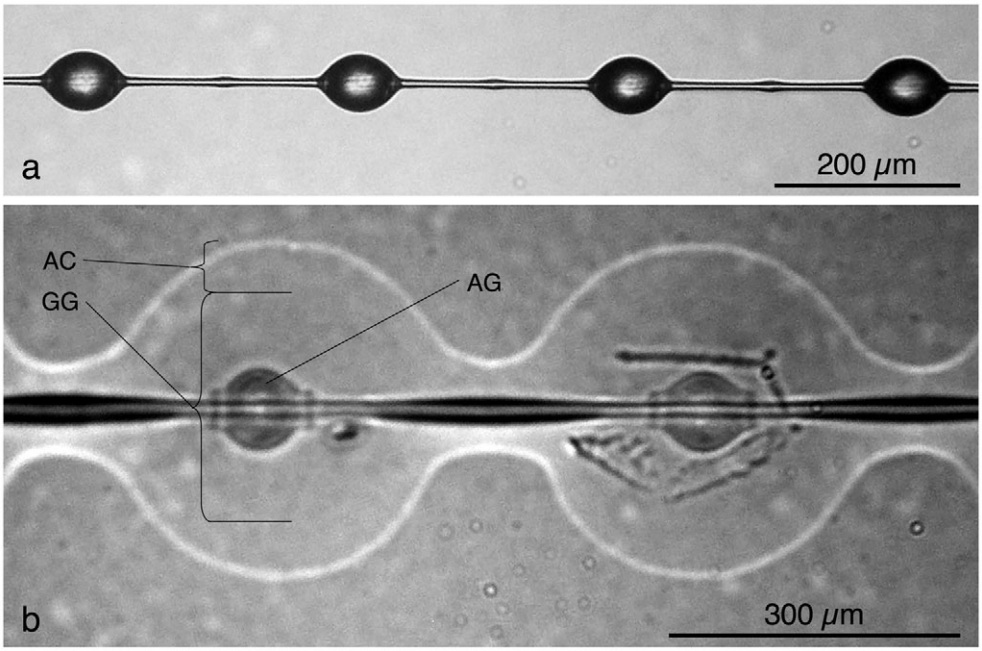

Fig. 1. (a) Suspended droplets of *Larinioides cornutus* viscous threads. (b) Flattened droplets showing a droplet's aqueous covering (AC), barely visible glycoprotein glue (GG) and anchoring granule (AG) regions (Opell and Hendricks, 2010).

that are considered to be hydrophilic (Choresh et al., 2009), it is probable that some of the atmospheric water initially attracted by the LMWCs in a droplet's outer aqueous covering is incorporated into the underlying glycoprotein as the water content of these two droplet regions comes into equilibrium. Nuclear magnetic resonance studies indicate that water molecules enhance viscous thread plasticity (Bonthrone et al., 1992). Therefore, we hypothesize that water uptake by glycoprotein increases droplet extensibility. We test this hypothesis by measuring the extensibility of viscous droplets at three humidity values representing observed environmental ranges and assess the impact of humidity on droplet adhesion by comparing the deflection of the axial lines that support these droplets. Our results provide the first evidence that droplet extensibility increases greatly as environmental humidity rises and indicate that this results from increased glycoprotein plasticity, not increased glycoprotein adhesion.

MATERIALS AND METHODS

Species studied and thread collecting

We studied the threads of *Larinioides cornutus* (Clerck 1757) (Family Araneidae) because the performance of this species' thread droplets has been thoroughly characterized (Sahni et al., 2010). We collected the webs of eight adult female spiders from a barn in the Whitethorn community of Montgomery County, VA, USA. The barn sheltered these spiders from rain and seasonal changes, allowing us to collect threads between 4 and 25 October 2010 after we had perfected our techniques using threads spun by other species. On each study day, a web sample was collected between 07:30 and 08:30 h and all photographs used to compute droplet volume and extensibility were taken by 12:00 h of the same day.

A spider's orb-web sample was collected on a 17 cm diameter aluminum ring with a bar across its center. Scotch® double-coated tissue tape (Tape 4101T; 3M, St Paul, MN, USA) applied to the 5 mm wide rim of the ring and bar secured threads at their native tensions. The ring was then transported to the laboratory in a closed container. Relative humidity (RH) and temperature were measured in the field when each web sample was collected using a Fisher Scientific digital hygrometer thermometer. Although we cannot establish that these conditions are those under which webs were constructed, these values provide a good index of humidity levels during the night and early morning hours when webs are constructed (Fig. 3). The mean (±s.e.m.) temperature at web sample collection was 10.15±1.22°C and the mean RH was 84.5±3.7%.

In the laboratory, we placed 4-mm-wide brass bars covered with double-sided carbon tape (product 77816, Electron Microscopy Sciences, Hatfield, PA, USA) across the rim of the ring and its center bar along the web's radial threads. This allowed us to collect short spans of capture thread without damaging other regions of the web sample. We collected individual threads using a pair of tweezers whose tips were covered with double-sided carbon tape and blocked open to accommodate the support spacing of thread samplers. This was done under a dissecting microscope by pressing the tweezers tips against a thread and cutting it free using iris scissors. This thread was then pressed against the raised supports on a microscope slide sampler and cut free of the tweezers. This sampler consisted of five rectangular brass U-shaped supports glued on their closed surface to a microscope slide and separated by a distance of 4.8 mm. The two upper rims of each support were covered with double-sided carbon tape.

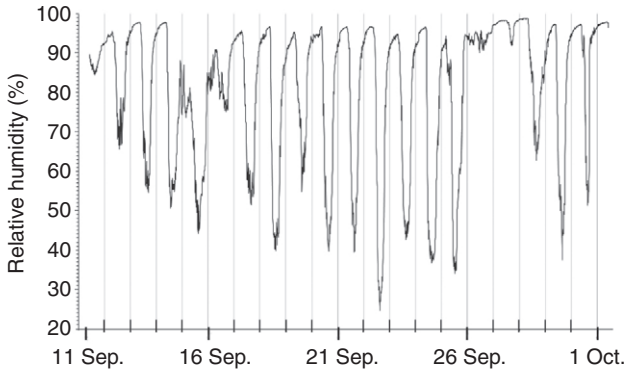

Fig. 2. Relative humidity recorded by a Hobo® data logger in 2009 at field site near where *L. cornutus* threads were collected for this study. The daily peaks reflect high evening through morning humidity levels and the valleys low mid-day humidity levels.

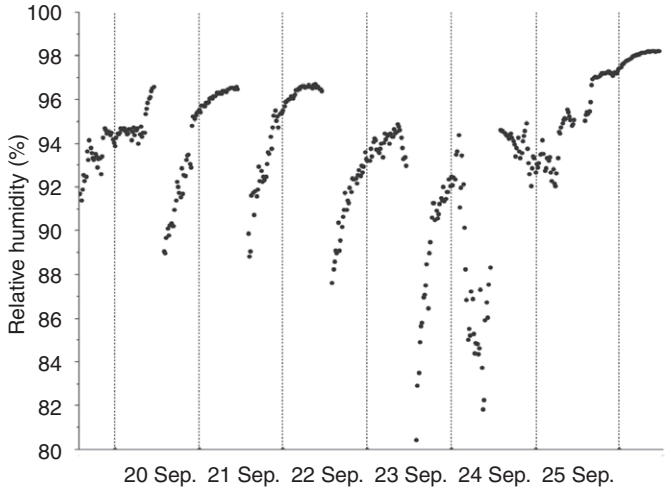

Fig. 3. Relative humidity during the 10:00–08:30 h time period of the 20–26 September time frame shown in Fig. 2, when daily humidity fluctuations were greatest. Dashed lines mark the 03:00 h midpoint of these time periods.

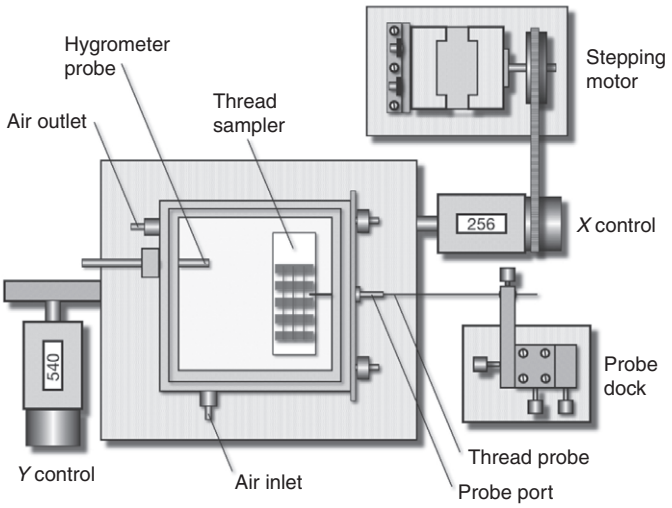

Fig. 4. Top view of the humidity-controlled chamber and mechanical control system, which features *X* and *Y*-stage manipulators with digital readouts.

When a series of droplets contacted the tip of a probe used to elongate droplets, adjacent droplets sometimes merged as they flattened on the probe or as droplets began to elongate. To ensure that the probe would contact only one droplet, we isolated an individual droplet near the center of each 4.8-mm-long thread span. To accomplish this, we first exhaled on the threads to temporarily more fully hydrate their droplets. This allowed the unwanted droplets to be more easily pushed to the side by the moistened tip of a small probe made from an insect minuten pin. This procedure did not appear to remove the thin aqueous covering of axial fibers in inter-droplet regions. After droplets had been moved, small secondary droplets, similar to those commonly found between the large primary droplets of many native threads, often re-formed in the regions where larger droplets had been.

Controlling humidity and observing threads

To control RH, thread samplers were placed inside a humidity chamber (Fig. 4), which incorporated a microscope slide holder, a port on the right side to allow entry of a probe, air inlet and outlet ports on the bottom and left upper sides, and a port near the center of the left side to hold the probe of a Fisher Scientific Instant Digital Hygrometer, whose readings were updated in less than 10 s. A sheet of anti-Newton glass resting on a Sorbothane gasket sealed the top of this aluminum chamber. Air drawn into this chamber by a small electric vacuum pump entered through a manifold equipped with valves that allowed us to select room air, desiccated air that had passed through a cylinder filled with silica gel beads, or humidified air that was drawn through an aquarium aerator submerged in distilled water before passing through a glass cylinder packed with Upsorb sheets (Diversified Biotech, Dedham, MA, USA) that were saturated with distilled water. One or two small Petri dishes with silica gel beads were placed in the chamber to help achieve and stabilize low RH values and a dish with a Kimwipe® saturated with distilled water was placed in the chamber to help achieve and stabilize high RH values. Small adjustments to RH were made by gently exhaling into a tube connected to the input port or by drawing in small volumes of room or desiccated air.

The probe entry port was mounted on a sliding plate sealed against the outer right side of the humidity chamber with vacuum grease and secured by thumbscrews (Fig. 4). This permitted the probe that we used to elongate droplets to be aligned with a droplet on different sectors of the slide sampler. After aligning the probe, tightening the thumbscrews and bringing the probe tip near a droplet, the probe was secured to a stationary holder, whose *X*,*Y*,*Z* alignment permitted probe docking. The chamber rested on the mechanical stage of a Mitutoyo FS60 inspection microscope (Mitutoyo America Corp., Aurora, IL, USA), which was equipped with a digital *X*,*Y* manipulator. In addition to being hand operated, the *X* drive on the right side of the stage was connected by a cog belt to a Vexta 2 phase, 0.9 deg per step, stepping motor (Oriental Motor U.S.A. Corp., Torrance, CA, USA) controlled by a Phidgets 1063 PhidgetStepper Bipolar 1 stepping motor controller (Calbary, Alberta, Canada), which was activated by a computer. This permitted a thread sample to be moved towards or away from the stationary probe at a constant speed. We slowly advanced a droplet toward the probe tip and, after it made contact, advanced the droplet an additional 500 µm to ensure adhesion. We next withdrew the chamber using the stepping motor, causing the droplet to be elongated at a velocity of 69.5 µm s^{-1}. Before each trial, the probe's tip was cleaned with 95% ethanol on a Kimwipe®.

We began a series of measurements by placing a microscope slide sampler with prepared droplets into the humidity chamber. Before photographing droplets and measuring their extensibility at 22°C, we first decreased the chamber's RH to a mean value of 17% (Table 1). We next raised RH to a mean value of 54% and finally, elevated RH to a mean value of 90%. Our preliminary studies of *Argiope aurantia* and *Verrucosa arenata* threads, whose droplets were much larger than those of *L. cornutus* (Opell and Hendricks, 2009), indicated that droplet volume comes into equilibrium with ambient humidity within a few minutes. In the present study it typically required 5–15 min for us to establish the desired RH, with the last few minutes being devoted to RH adjustments of only a few percent. Following this, we located droplets, on strands, focused the microscope and captured images, recording the RH immediately after doing so. After capturing these still images, we aligned the

probe used to extend droplets, set up the camera's video options and began capturing images of extending droplets, again recording the RH at which extension was accomplished. Given the length of these procedures, we are confident that the volumes of the droplets that we photographed had ample time to come into equilibrium with the recorded ambient RH.

Droplet size and extensibility

The Mitutoyo microscope that we used to observe and photograph droplets was equipped with epi-illumination through its 2, 5, 10 and 20× objectives. The microscope's two-power zoom knob was retrofitted with a scale that allowed its magnification to be calibrated and recorded at a resolution of 0.0125×. Using an attached Canon Powershot S5IS digital camera, we first captured still images of two of an individual's droplets at a given test RH and then captured video images (60 frames s^{-1}) of each of these droplets as they were extended. We previewed each video of elongating droplets and captured the frame immediately prior to a droplet's release from the probe tip (Fig. 5).

When measuring images of native droplets taken at each test RH with ImageJ, we used an image of a stage micrometer taken at the same magnification for scale. When measuring images of extending droplets, we used the 413 µm width of the flange at the probe's tip as a scale (Fig. 5). We measured the length (parallel to the thread's axial lines) and width of native droplets and used these measurements to determine droplet volume (V_D) according to the following formula (Opell and Schwend, 2007):

$$V_D = (2\pi W_D^2 L_D) / 15, \quad (1)$$

where W_D is the droplet width and L_D is the droplet length. In addition to simple measurements of droplet extension at each RH, we computed droplet extension per droplet volume, an index that we term relative droplet extension. In determining an individual's two droplet dimensions, volumes and extensions were averaged, providing one set of measurements for each test RH. Relative droplet extension values were determined for each of an individual's two droplets and averaged for an individual. Consequently, for each RH value, the grand mean values reported in Table 1 differ from those computed by dividing mean droplet extension by mean droplet volume. We analyzed these values using JMP (SAS Institute, Cary, NC, USA), considering $P \leq 0.05$ as significant.

Droplet extensibility *vs* droplet adhesion

An alternative to our hypothesis that increased humidity causes increased droplet extensibility is that increased humidity increases droplet adhesion, which, in turn, allows droplets to extend farther before they release. Although we were not able to directly measure the force on extending droplets, we were able to assess this hypothesis by measuring the deflection of the axial lines on which droplets were found. Axial lines of the same 4.8 mm length supported all droplets and all droplets were located near the centers of their lines. Therefore, as force increases on a droplet, the angle formed by the axial lines extending on either side of a droplet should decrease from the no-load condition of 180 deg. For six individuals we were able to measure this angle in the terminal droplet extension images for the three humidity levels and in an additional individual for the 17 and 54% humidity levels. We used these angle measurements to test the hypothesis that force on a droplet increased as humidity increased, as indicated by a decrease in the angle formed by the axial line on either side of an elongating droplet. As in droplet extension, we first computed the mean angle of an individual's axial lines at each test humidity level and then statistically tested differences in angles among humidity levels.

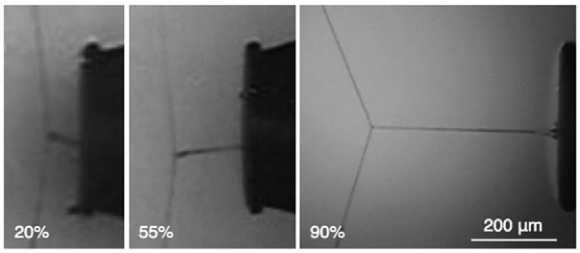

Fig. 5. Droplets of *L. cornutus* individual 7 at their maximum extensions under three relative humidity values: 20, 55 and 90%.

RESULTS

Table 1 presents mean values for droplet dimension and volume, droplet extension and relative droplet extension at the three test RH values and reports *P*-values for ANOVA tests of differences in each of these features among the three humidity levels. Each individual's mean droplet extension increased from 17 to 54% and from 54 to 90% RH. Mean individual relative droplet extension also increased with RH except for two instances from 17 to 54% RH and one instance from 54 to 90% RH. An increase in RH from 17 to 54% increased mean (±s.e.m.) individual droplet extension by 164.75±37.79 µm and relative droplet extension by $2.48\times10^2\pm1.05\times10^2$ µm µm^{-3}. An increase in RH from 54 to 90% increased extension by 571.75±184.53 µm and relative droplet extension by $8.81\times10^2\pm4.20\times10^2$ µm µm^{-3}. This increase in droplet extension was significant (ANOVA, P=0.0485), but that of relative droplet extension was not (ANOVA, P=0.1663). When droplet extension and relative droplet extension at 54 and 90% RH were expressed as percent increases over the values measured at 17% RH (Fig. 6), these sequential changes differed for both extension and relative extension (ANOVA, P=0.0316 and 0.0292, respectively).

Table 1. Mean droplet dimensions and extensions at the three experimental relative humidity levels and results of ANOVAs on the effect of the relative humidity levels on these variables

	Relative humidity (%)			
	17±1.5	54±0.7	90±0.2	*P*
Droplet length (µm)	28.5±4.1	30.1±3.9	32.0±4.0	0.8286
Droplet width (µm)	19.7±2.9	21.3±2.8	23.3±2.9	0.6808
Volume (µm^3)	6161±2362	8296±3032	10,664±4045	0.6202
Droplet extension (µm)	114±19	279±46	851±203	0.0008
Relative droplet extension ($\times10^2$ µm µm^{-3})	4.07±1.13	6.55±1.43	15.35±4.44	0.0224

Values are means ± 1 s.e.m.; N=8 for all measurements.

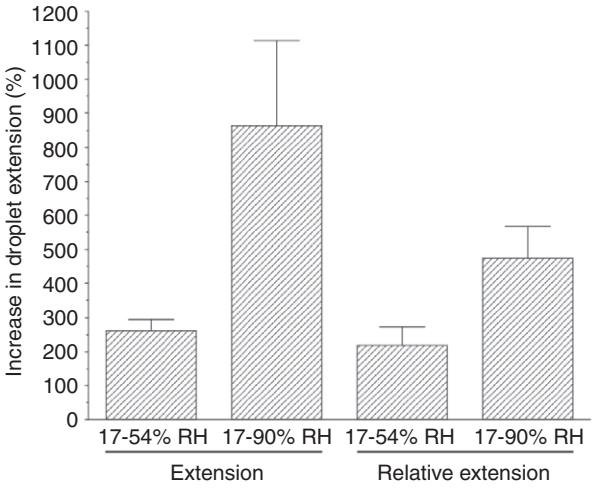

Fig. 6. Histogram of the mean (±1 s.e.m.) percent increases in droplet extension and relative droplet extension from 17 to 54% and from 17 to 90% relative humidity (RH).

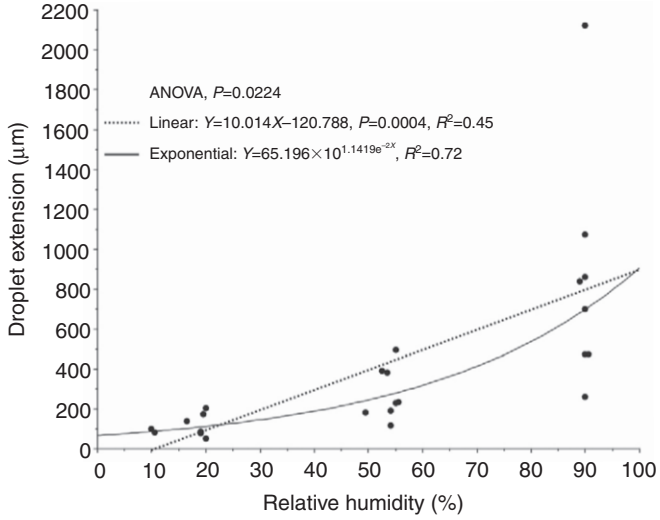

Fig. 7. ANOVA and regressions of test RH and droplet extension.

Both droplet extensibility and relative droplet extension were normally distributed for each of the three RH levels (Shapiro–Wilk *W*-test, low to high RH values, P=0.42, 0.41, 0.07 and 0.48, 0.81, 0.14, respectively). ANOVA tests show that mean RH affects both droplet extension and relative droplet extension, both when the mean RH values of 17, 54 and 90% are used as independent variables (Table 1) and when individual test RH values are used (Figs 7 and 8). As these test RH values differed slightly among individuals, the extension and relative extension of droplets can be regressed against the RH at which these indices were measured (Figs 7 and 8). These linear regressions are significant, although exponential regressions improved the model's R^2, suggesting, along with the pattern of percent increase in droplet extension (Fig. 6), that droplet extension increases progressively as RH increases.

The mean deflection angles of axial lines at maximum droplet extension for 17, 54 and 90% RH values were 149.9±5.4 deg, N=7; 145.1±6.4 deg, N=7; and 161.0±4.4 deg, N=6, respectively. These angles were normally distributed for each humidity level (Shapiro–Wilk *W*-test, P=0.31, 0.30 and 0.98, respectively) and did not differ among humidity levels (ANOVA, P=0.1591).

Although we collected threads during a period of only 21 days, this period occurred near the end of the spiders' lives. Therefore, to determine whether seasonal change contributed to the variance in our data, we regressed collection day against mean droplet volume, mean droplet extension, standard deviation of mean extension, collection temperature, collection RH and collection dew point. All relationships were insignificant ($0.0596<P<0.56$), although RH had a P-value of 0.0596, perhaps as a result of a slight, but erratic, trend of decreasing temperature. However, RH at the time of web sample collection was unrelated to droplet extension (P=0.9094). Consequently, we find no evidence that temperature or RH at the time of web construction affected the thread features that we measured.

DISCUSSION

As hypothesized, droplet extensibility increased with humidity. This is consistent with increased glycoprotein plasticity resulting from water uptake by charged amino acids (Choresh et al., 2009). The alternative explanation that hydration increased glycoprotein adhesion, allowing droplets to extend farther before they released from the probe, was not supported by changes in deflection of the supporting axial lines. In fact, the only noticeable trend was decreased axial line deflection at the highest humidity. This is consistent with evidence that the water content of viscous threads does not affect their adhesion (Opell and Hendricks, 2009), that capillary forces contribute very little to viscous thread adhesion (Sahni et al., 2010) and that the polar component of a material's surface energy, which is most likely to interact with water in viscous droplets, does not make a detectable contribution to the adhesion of viscous threads (Opell et al., 2011).

As both the outer aqueous covering of a droplet and its inner glycoprotein glue contain hydrophilic components (Vollrath et al., 1990; Townley et al., 1991; Edmonds and Vollrath 1992; Choresh et al., 2009), water absorbed from the atmosphere must be distributed between these two regions, reaching new equilibria as RH changes. This may explain why expressing droplet extension relative to droplet volume proved to be a statistically less satisfactory way of gauging the extension of droplets (Figs 7 and 8). If glycoprotein

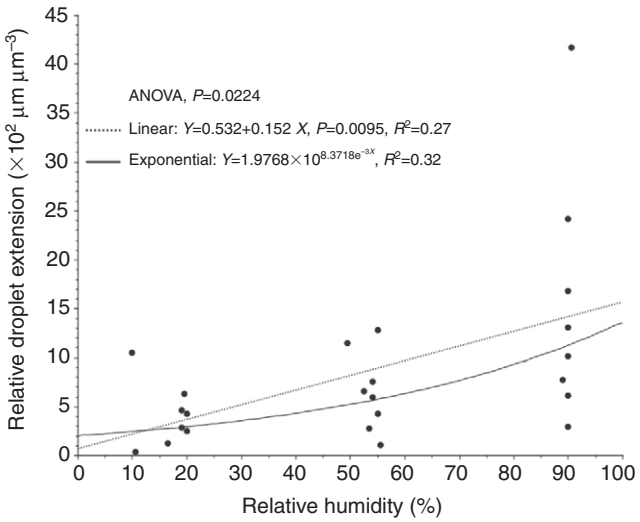

Fig. 8. ANOVA and regressions of test RH and relative droplet extension (droplet extension per volume).

molecules incorporate less water than the droplets' aqueous covering, then a volume-related index of droplet extensibility would under-represent droplet extension. This trend is suggested when the histograms (Fig. 6) and regressions (Figs 7 and 8) of droplet extension and relative droplet extension are compared.

The force required to overcome a viscous thread's adhesion is the sum of the forces required to extend the thread's axial fibers, elongate its elastic glycoprotein glue and overcome the adhesion of this glue (Sahni et al., 2010). As discussed previously, it seems unlikely that changes in humidity directly affect glycoprotein adhesion. Likewise, as axial fibers within and between droplets are covered by aqueous material, changes in humidity probably have minimal impact on their hydration. This leaves changes in glycoprotein extensibility as the principal humidity-related influence on thread adhesion. The work required to stretch glycoprotein is the product of its resistance to deformation and the distance over which it must be elongated. If droplets stretch further because their glycoproteins offer less resistance to deformation, then the work of stretching droplets may not change with humidity. However, increased glycoprotein extensibility has the potential to alter thread stickiness in two other ways. If the outer droplets of a thread extend further under high humidity, then the thread's axial fibers would assume a more acute angle with the surface to which the thread adhered. This would increase the force on the outermost droplets of the contacting thread strand, reduce the thread's ability to recruit adhesion from more interior droplets and cause the thread to release at a lower force than it would at a lower humidity. Increased glycoprotein elasticity might also increase the tendency for glycoprotein to be withdrawn from droplet–surface interfaces as droplets stretch, thereby reducing a thread's stickiness by reducing the footprints of its adhering droplets.

The potential for environmental humidity to affect viscous thread adhesion suggests that an orb web's prey retention ability may change over the course of a day. As orb webs intercept a great diversity of insects, which are characterized by different surface features (Opell and Schwend, 2007), the impact of droplet extensibility may extend beyond simple thread adhesion. More plastic droplets may retain some insects better and stiffer droplets may retain others better. If this is indeed the case, then selection may have adapted a thread's hygroscopicity and droplet extensibility to the humidity regime of a species' habitat and, in some cases, to particular types of insect prey.

ACKNOWLEDGEMENTS

Harold Schwend provided helpful comments on this paper.

REFERENCES

Agnarsson, I. and Blackledge, T. A. (2009). Can a spider web be too sticky? Tensile mechanics constrains the evolution of capture spiral stickiness in orb-weaving spiders. *J. Zool.* **278**, 134-140.

Blackledge, T. A. and Hayashi, C. Y. (2006a). Silken toolkits: biomechanics of silk fibers spun by the orb web spider *Argiope argentata* (Fabricius 1775). *J. Exp. Biol.* **209**, 2452-2461.

Blackledge, T. A. and Hayashi, C. Y. (2006b). Unraveling the mechanical properties of composite silk threads spun by cribellate orb-weaving spiders. *J. Exp. Biol.* **209**, 3131-3140.

Blackledge, T. A. and Zevenbergen, J. M. (2006). Mesh width influences prey retention in spider orb webs. *Ethology* **112**, 1194-1201.

Bonthrone, K. M., Vollrath, F., Hunter, B. K. and Sanders, J. K. M. (1992). The elasticity of spiders' webs is due to water-induced mobility at a molecular level. *Proc. R. Soc. Lond. B* **248**, 141-144.

Chacón, P. and Eberhard, W. G. (1980). Factors affecting numbers and kinds of prey caught in artificial spider webs with considerations of how orb webs trap prey. *Bull. Br. Arachnol. Soc.* **5**, 29-38.

Choresh, O., Bayarmagnai, B. and Lewis, R. V. (2009). Spider web glue: two proteins expressed from opposite strands of the same DNA sequence. *Biomacromolecules* **10**, 2852-2856.

Coddington, J. A. (1989). Spinneret silk spigot morphology: evidence for the monophyly of orb-weaving spiders, Cyrtophorinae (Araneidae), and the group Theridiidae plus Nesticidae. *J. Arachnol.* **17**, 71-96.

Edmonds, D. and Vollrath, F. (1992). The contribution of atmospheric water vapour to the formation and efficiency of a spider's web. *Proc. R. Soc. Lond. B* **248**, 145-148.

Gosline, J. M., Pollak, C. C., Guerette, P. A., Cheng, A., DeMont, M. E. and Denny, M. W. (1994). Elastomeric network models for the frame and viscid silks from the orb web of the spider *Araneus diadematus*. In *Silk Polymers, Materials Science and Biotechnology* (ed. D. Kaplan, W. Adams, B. Farmer and C. Viney), pp. 328-341. Washington, DC: American Chemical Society.

Guinea, G. V., Cerdeira, M., Plaza, G. R., Elices, M. and Pérez-Rigueiro, J. (2010). Recovery in viscid line fibers. *Biomacromolecules* **11**, 1174-1179.

Opell, B. D. and Hendricks, M. L. (2007). Adhesive recruitment by the viscous capture threads of araneoid orb-weaving spiders. *J. Exp. Biol.* **210**, 553-560.

Opell, B. D. and Hendricks, M. L. (2009). The adhesive delivery system of viscous prey capture threads spin by orb-weaving spiders. *J. Exp. Biol.* **212**, 3026-3034.

Opell, B. D. and Hendricks, M. L. (2010). The role of granules within viscous capture threads of orb-weaving spiders. *J. Exp. Biol.* **213**, 339-346.

Opell, B. D. and Schwend, H. S. (2007). The effect of insect surface features on the adhesion of viscous capture threads spun by orb-weaving spiders. *J. Exp. Biol.* **210**, 2352-2360.

Opell, B. D., Markley, B. J., Hannum, C. D. and Hendricks, M. L. (2008). The contribution of axial fiber extensibility to the adhesion of viscous capture threads spun by orb-weaving spiders. *J. Exp. Biol.* **211**, 2243-2251.

Opell, B. D, Schwend, H. S. and Vito, S. T. (2011). Constraints on the adhesion of viscous threads spun by orb-weaving spiders: The tensile strength of glycoprotein glue exceeds its adhesion. *J. Exp. Biol.* **214**, 2237-2241.

Peters, H. M. (1986). Fine structure and function of capture threads. In *Ecophysiology of Spiders* (ed. W. Nentwig), pp. 187-202. New York: Springer Verlag.

Peters, H. M. (1995). Ultrastructure of orb spiders' gluey capture threads. *Naturwissenschaften* **82**, 380-382.

Platnick, N. I. (2011). *The World Spider Catalog,* Version 11.5. American Museum of Natural History, online at http://research.amnh.org/iz/spiders/catalog. DOI:10.5531/db.iz.0001.

Sahni, V., Blackledge, T. A. and Dhinojwala, A. (2010). Viscoelastic solids explain spider web stickiness. *Nat. Commun.* **1**, 19.

Savage, K. and Gosline, J. (2008). The role of proline in the elastic mechanism of hydrated spider silks. *J. Exp. Biol.* **211**, 1948-1957.

Sensenig, A., Agnarsson, I. and Blackledge, T. A. (2010). Behavioral and biomaterial coevolution in spider orb webs. *J. Evol. Biol.* **23**, 1807-2029.

Swanson, B. O., Blackledge, T. A. and Hayashi, C. Y. (2007). Spider capture silk: performance implications of variation in an exceptional biomaterial. *J. Exp. Zool. A* **307**, 654-666.

Tillinghast, E. K., Townley, M. A., Wight, T. N., Uhlenbruck, G. and Janssen, E. (1993). The adhesive glycoprotein of the orb web of *Argiope aurantia* (Araneae, Araneidae). *Mat. Res. Soc. Symp. Proc.* **292**, 9-23.

Townley, M. A., Bernstein, D. T., Gallagher, K. S. and Tillinghast, E. K. (1991). Comparative study of orb-web hygroscopicity and adhesive spiral composition in three araneid spiders. *J. Exp. Zool.* **259**, 154-165.

Vollrath, F. (1992). Spider webs and silks. *Sci. Am.* **266**, 70-76.

Vollrath, F. and Edmonds, D. (1989). Modulation of the mechanical properties of spider silk by coating with water. *Nature* **340**, 305-307.

Vollrath, F. and Tillinghast, E. K. (1991). Glycoprotein glue beneath a spider web's aqueous coat. *Naturwissenschaften* **78**, 557-559.

Vollrath, F., Fairbrother, W. J., Williams, R. J. P., Tillinghast, E. K., Bernstein, D. T., Gallagher, K. S. and Townley, M. A. (1990). Compounds in the droplets of the orb spider's viscid spiral. *Nature* **345**, 526-528.

Work, R. W. (1981). A comparative study of the supercontraction of major ampullate silk fibers of orb-web-building spiders (Araneae). *J. Arachnol.* **9**, 299-308.

Work, R. W. (1982). A physico-chemical study of the supercontraction of spider major ampullate silk fibers. *Text. Res. J.* **52**, 349-356.